

Electrochemical Cysteine Sensor on Novel Ruthenium Based Ternary Catalyst

Hilal Kivrak^{1,2,*}, Kadir Selçuk², Omer Faruk Er², Nahit Aktas^{2,3*}

¹ Eskisehir Osmangazi University, Faculty of Engineering and Architectural Sciences, Department of Chemical Engineering, Eskişehir, 26040 Turkey

² Van Yuzuncu Yil University, Faculty of Engineering, Department of Chemical Engineering, Van, 65000 Turkey

³ Kyrgyz-Turk Manas University, Faculty of Engineering, Department of Chemical Engineering, Bishkek, Kyrgyzstan

*E-mail: hilalkivrak@gmail.com, nahit.aktas@manas.edu.kg, naktas@yyu.edu.tr

Received: 21 January 2021 / Accepted: 16 March 2021 / Published: 31 March 2021

At present, a voltammetric L-Cystein (Cys) sensor is developed based on carbon nanotube (CNT) supported Ru-Mo-Pd trimetallic catalyst modified glassy carbon electrodes (GCE). Firstly, Ru-Mo/CNT catalysts are prepared via sodium borohydride reduction method and following this Ru-Mo/CNT modified GCE electrode is prepared and Pd electrodeposition at varying Pd concentrations is performed to obtain Ru-Mo-Pd/CNT catalysts. Ru-Mo-Pd/CNT catalyst is characterized by TEM and SEM-EDX. Characterization results reveal that Ru-Mo-Pd/CNT catalyst is successfully synthesized. For electrochemical measurements, GCE is modified with Ru-Mo-Pd/CNT catalysts and electrochemical behavior of the modified GCE is investigated by cyclic voltammetry, differential pulse voltammetry, electrochemical impedance spectroscopy. Ru-Mo-Pd/CNT at 0.0152 mM Pd concentration modified GCE electrode have the best Cys electrooxidation activity. Hence, further electrochemical measurements to determine sensitivity, limit of detection, intereference study, and real sample are performed on Ru-Mo-Pd/CNT at 0.0152 mM Pd concentration modified GCE electrode. This sensor has a wide linear response within the range of 5–200 μM with high current sensitivity 0.136 $\mu\text{A}/\mu\text{M}$ and 0.1 μM as lowest detection limit at (S/N=3) signal to noise ratio. Interference studies reveal that Ru-Mo-Pd/CNT sensor is not affected by common interfering species. This novel study reports a strategy to sense Cys on Ru/CNT modified GCE electrode.

Keywords: Cysteine; Ruthenium; Palladium; Molybdenum; electrochemical; sensor

1. INTRODUCTION

Proteins contain carbon (50-55%), hydrogen (6-7%), nitrogen (12-19%), sulfur (0.2-3.0%), and oxygen (20-23%). Furthermore, proteins contain P, Fe, Zn, and Cu elements. The most important feature

of proteins is that they contain nitrogen and with this feature they differ from fats and carbohydrates. Proteins contain different numbers and amino acids in the sequence, have different structures and thousands of types of protein fulfil a range of functions. The smallest building block of proteins is called as amino acid. Amino acids are essential for vital processes in the body such as the synthesis of proteins, hormones, and neurotransmitters. Amino acids coexist with lipids in the membrane of cells and are also involved in the structure of hormones and enzymes. Amino acids are organic compounds containing amino ($-\text{NH}_3^+$), carboxyl ($-\text{COO}^-$), and side chain (R) groups in their structure. There is an average of 20 amino acids; they fall into two different groups as essential and non-essential amino acids. Each amino acid has the same nitrogen number but different carbon numbers. Essential amino acids are isoleucine, leucine, valine, lysine, methionine, phenylalanine, threonine, and tryptophan. Non-essential amino acids include alanine, arginine, asparagine, aspartic acid, cysteine, glutamic acid, glutamine, glycine, proline, serine, and tyrosine. These are amino acids that can be made from essential organic substances in the body and are usually not essential, except in times of illness and stress [1-18].

Cysteine (Cys) is a semiessential proteinogenic amino acid with the formula of $\text{HO}_2\text{CCH}(\text{NH}_2)\text{CH}_2\text{SH}$. The thiol side of Cys usually participates in enzymatic reactions, as a nucleophile [1-9]. Cys is found in high protein foods. Cys can usually be synthesized by the human body under normal physiological conditions if a sufficient quantity of methionine is available. It is commonly used in the food, pharmaceutical, and personal care industries today. With code E920 code, the aforementioned Cys can be used especially for bread in the food industry to improve the quality of some bakery products. Industrially, Cys is produced from human or animal hair mainly using acid or as a result of alkali hydrolysis [10-18].

Sensitive detection of Cys is important to develop effective nanomaterials and methods for Cys. There are various techniques to determine the Cys level, such as spectrometric chromatographic separation [19-21], colorimetric [22-28], and electrochemical methods [1-9]. Electrochemical methods have important advantages such as simple operation, cheap instruments, easy miniaturization, and acceptable selectivity [29-38]. For the electrochemical detection of Cys, selection of the electrode material is vital to construct sensitive and flexible Cys sensors for determination of Cys. Ahmad and coworkers [1] reported that elbow shaped Sb-doped ZnO nanowires were synthesized by thermal evaporation, characterized, and their L-cystein sensor sensitivities were defined. They found that the response current of L-CySH oxidation at the Sb-doped ZnO nanowires modified GCE electrode was much higher than that of the bare GCE and ZnO/GCE electrodes with a reproducible sensitivity of $400 \text{ nA}\mu\text{M}^{-1}$, a detection limit of $0.025 \mu\text{M}$ and a linear range of 0.075 to $100 \mu\text{M}$. Likewise, Xiao et al. [2] studied on a novel one-dimensional (1-D) caterpillar-like manganese dioxide-carbon ($\text{MnO}_2\text{-C}$) nanocomposite synthesis with high specific surface area ($200 \text{ m}^2\text{g}^{-1}$) and favourable conductivity. The nanostructured $\text{MnO}_2\text{-C}$ composite modified GCE had high catalytic currents showing a good linear relationship with that of the L-Cys concentration in the range of $0.5\text{--}680 \mu\text{M}$ ($R = 0.9986$), with a low detection limit of 22 nM . At another study performed by Silva and Coworkers, the preparation of an amperometric sensor based on a functional platform to complex copper ions on MWCNTs modified with poly-4-vinylpyridine through an *in situ* polymerization for electrocatalytical detection of Cys was described. One noted that the analytical curve showed a linear response range for detecting Cys in concentrations from $5\text{--}60 \mu\text{mol L}^{-1}$. The detection and quantification limits obtained were 1.50 and 5.00

$\mu\text{mol L}^{-1}$, respectively with a response time of 0.10 s at an applied potential of 150 mV vs SCE [3]. Similarly, cobalt tetraaminophthalocyanine (CoTAPc)/the MWCNTs were employed as Cys electrochemical sensor and results revealed that this material was good electrochemical sensor with a limit of detection of $2.8 \cdot 10^{-7}$ M [4]. Literature studies reveal that few studies have been carried out about the sensitive determination of Cys via electrochemical techniques [1-9]. To commercialize this sensor, new electrode materials should be developed. In light of this literature review, we aimed to develop a carbon-supported Ru-Mo-Pd catalyst and employ it as a Cys sensor to obtain a sensitive electrochemical Cys sensor. Carbon-based electrodes are widely used as electrochemical sensors due to the wide range of potential with lower background current, low cost, and chemical inertness [30, 34].

In the present research, MWCNT-supported Ru-Mo-Pd nanocatalysts were prepared by the sodium borohydride reduction method. In order to determine the crystal and electronic properties of these nanocatalysts, advanced surface analytical techniques such as inductively coupled plasma mass spectrometry transmission electron microscopy (TEM) and scanning electron microscopy coupled with electron x-ray diffraction (SEM-EDX) were carried out. For electrochemical measurements, GCE was modified with Ru-Mo-Pd/MWCNT catalysts and the electrochemical behavior of the modified GCE was examined by CV, DPV, and EIS. These results revealed that Ru-Mo-Pd/MWCNT-modified GCE has high sensitivity. Interference studies and real sample measurements were also carried out using Ru-Mo-Pd/MWCNT-modified GCE. Real sample measurements were carried out to determine Cys in a drug sample.

2. EXPERIMENTAL

Ru-Mo/MWCNT catalysts containing Ru (3 wt% per gram support) were synthesized with the NaBH_4 reduction method by using ruthenium(III) nitrosyl nitrate solution ($\text{Ru}(\text{NO})(\text{NO}_3)_x(\text{OH})_y$) as Ru precursor and molybdenum(VI) dichloride dioxide (MoO_2Cl_2) as Mo metal precursor. The detailed procedure was given in our previous studies [39-50]. To obtain Ru-Mo-Pd/MWCNT catalyst, 5 mg Ru-Mo-Pd/MWCNT catalyst was dispersed in Nafion 117 solution and 5 mL of this solution was dropped on the GCE and then this electrode was dipped in the Pd precursor of potassium tetrachloropalladate (II) (K_2PdCl_4 , 99.99%) containing 0.5 M H_2SO_4 at various concentrations. By employing CV, electrochemical deposition of Pd on Ru-Mo/MWCNT was carried out. Finally, Ru-Mo-Pd/MWCNT catalysts were obtained. Trimetallic Ru-Mo-Pd/MWCNT catalyst was characterized by SEM-EDX and TEM. TEM was performed on a Hitachi HighTech HT7700 high resolution-transmission electron microscope operating at 120 kV and a scanning electron microscope was used to obtain particle size and surface metal distribution [51, 52].

Electrochemical measurements were carried out for trimetallic Ru-Mo-Pd/MWCNT catalysts. Electrochemical measurements were completed with Ru-Mo-Pd/MWCNT-modified GCEs. Cys electrooxidation measurements were carried out using CV and DPV. CVs on Ru-Mo-Pd/MWCNT-modified GCEs were obtained with a scan rate of 100mV s^{-1} in 0.1M PBS with 10 mM Cys and potential range from -1 to 1 V under stirred conditions at room temperature (23 ± 2 °C). The effect of pH was examined for the electrocatalytic activity of Cys. CVs were obtained by using PBS prepared at different

pHs (5, 7.2, and 10) and adding 5 mM Cys. The effect of Cys concentration on the electrocatalytic activity of Cys was examined on trimetallic Ru-Mo-Pd/MWCNT-modified GCEs. The effect of scan rate on the electrocatalytic activity of Cys was examined on Ru-Mo-Pd/MWCNT-modified GCE. Cyclic voltammograms were obtained in 5 mM Cys PBS (pH=10) at 10-300 mV s⁻¹ scan rate. Furthermore, DPV measurements were carried out on Ru-Mo-Pd/MWCNT-modified GCE. The calibration plot of DPV curves was obtained by plotting the maximum current versus concentration values. From the slope of this calibration curve, sensitivity of the sensor was predicted. The electrochemical impedance spectrum was obtained on Ru-Mo-Pd/MWCNT-modified GCE at varying potentials in 0.1 M PBS (pH=10) and 5 mM Cys. The frequency range and signal amplitude were adjusted from 0.02–100,000 Hz and 10 mV, respectively.

For the interference study, CV and EIS measurements were obtained on Ru-Mo-Pd/MWCNT-modified GCE. Interference by D-glucose, uric acid, L-Tyrosine, L-Tryptophane, and H₂O₂ were examined at 0.6 V potential.

Real sample measurements were completed by detecting Cys in acetylcysteine effervescent tablets under optimal conditions with DPV. For this, 1 mg acetylcysteine was transferred into a 50 mL volumetric flask containing 0.1 M PBS solution at pH=10. Employing this stock solution, 1.5 mM acetylcysteine was prepared by diluting this solution and the response of the sensor was obtained in this solution. Then, 1.5 mM of acetylcysteine was added in the real sample solution and the response of the sensor was recorded again.

3. RESULTS AND DISCUSSION

3.1. Characterization of 3% RuMoPd/MWCNT catalyst

The distribution, morphology, and particle size of Ru, Mo, and Pd nanoparticles on the MWCNT were determined with TEM. TEM images and particle size distribution histograms for 3% Ru-Mo-Pd/MWCNT catalyst are presented in Figure 1. Ru, Mo, and Pd metals with spherical-shaped nanoparticles are clearly seen to be dispersed over MWCNT (Fig. 1). Moreover, nanoparticles were distributed over MWCNT with low agglomeration. The particle size calculated from TEM images of 3% Ru-Mo-Pd/MWCNT catalyst was found to be between 8-9 nm (Fig. 1e and f). In addition, the morphology of 3% Ru-Mo-Pd/MWCNT catalyst was examined with SEM-EDX. SEM images of 3% Ru-Mo-Pd/MWCNT catalyst are depicted in Figure 2. It is clearly observed in Fig. 2c that Ru, Mo, and Pd nanoparticles are well bonded and distributed on the structure of MWCNT. As a result, SEM and TEM images of 3% Ru-Mo-Pd/MWCNT catalyst revealed that the 3% Ru-Mo-Pd/MWCNT catalyst was prepared successfully. Furthermore, particles were attached inside the MWCNTs. EDX results showed that homogeneous distribution of Ru, Mo, and Pd nanoparticles was exhibited (Fig. 2d).

Elemental mapping of the 3% Ru-Mo-Pd/MWCNT catalyst is shown in Figure 3. These results demonstrate good distribution of Ru, Mo, and Pd nanoparticles on the MWCNT support material.

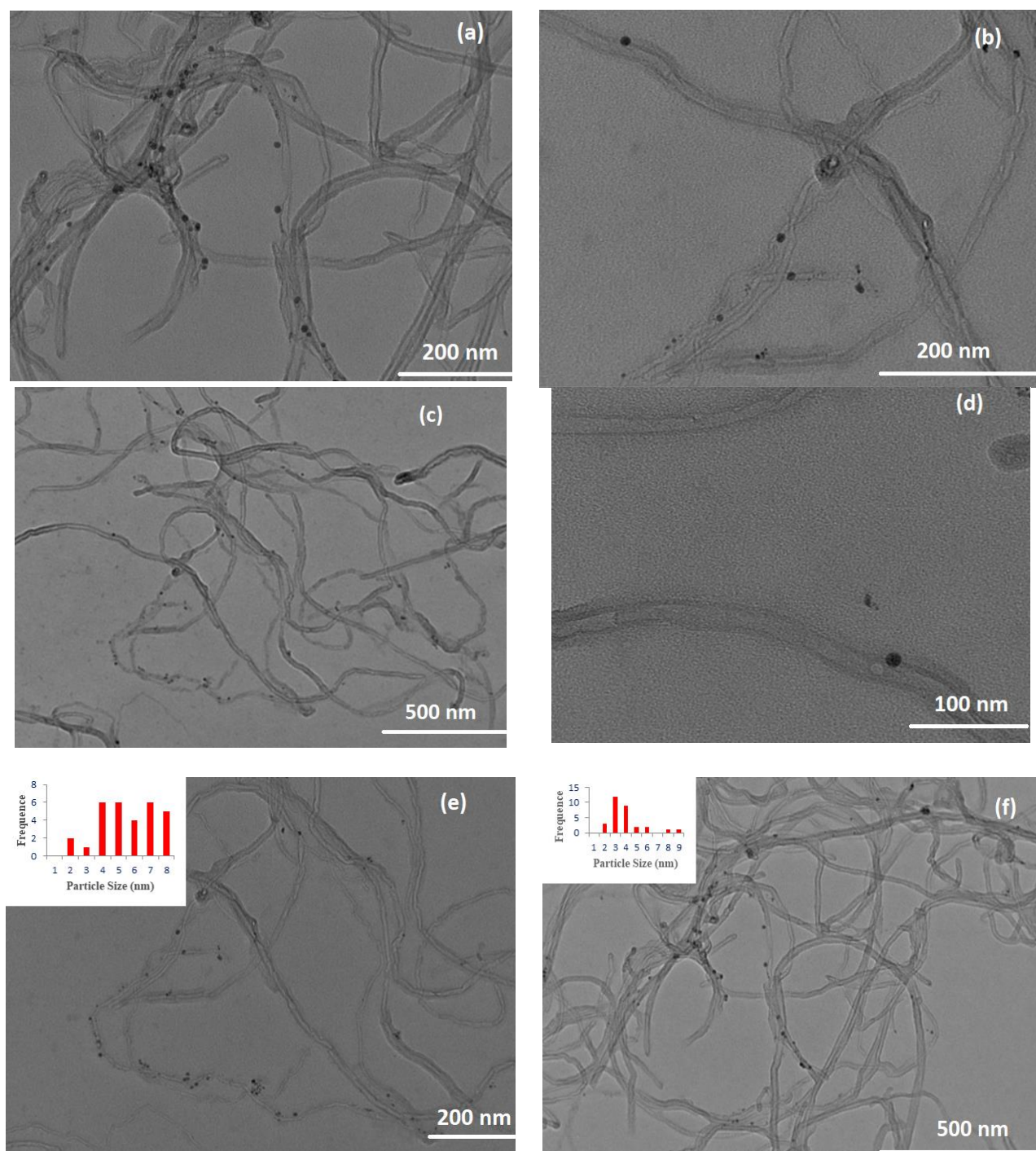


Figure 1. TEM images at different resolutions as (a-b) 200 nm, (c) 500 nm, (d) 100 nm, (e) 200 nm (insert graph: Particle size vs frequency graph), and (f) 500 nm (insert graph: Particle size vs frequency graph) for 3% Ru-Mo-Pd/MWCNT catalyst.

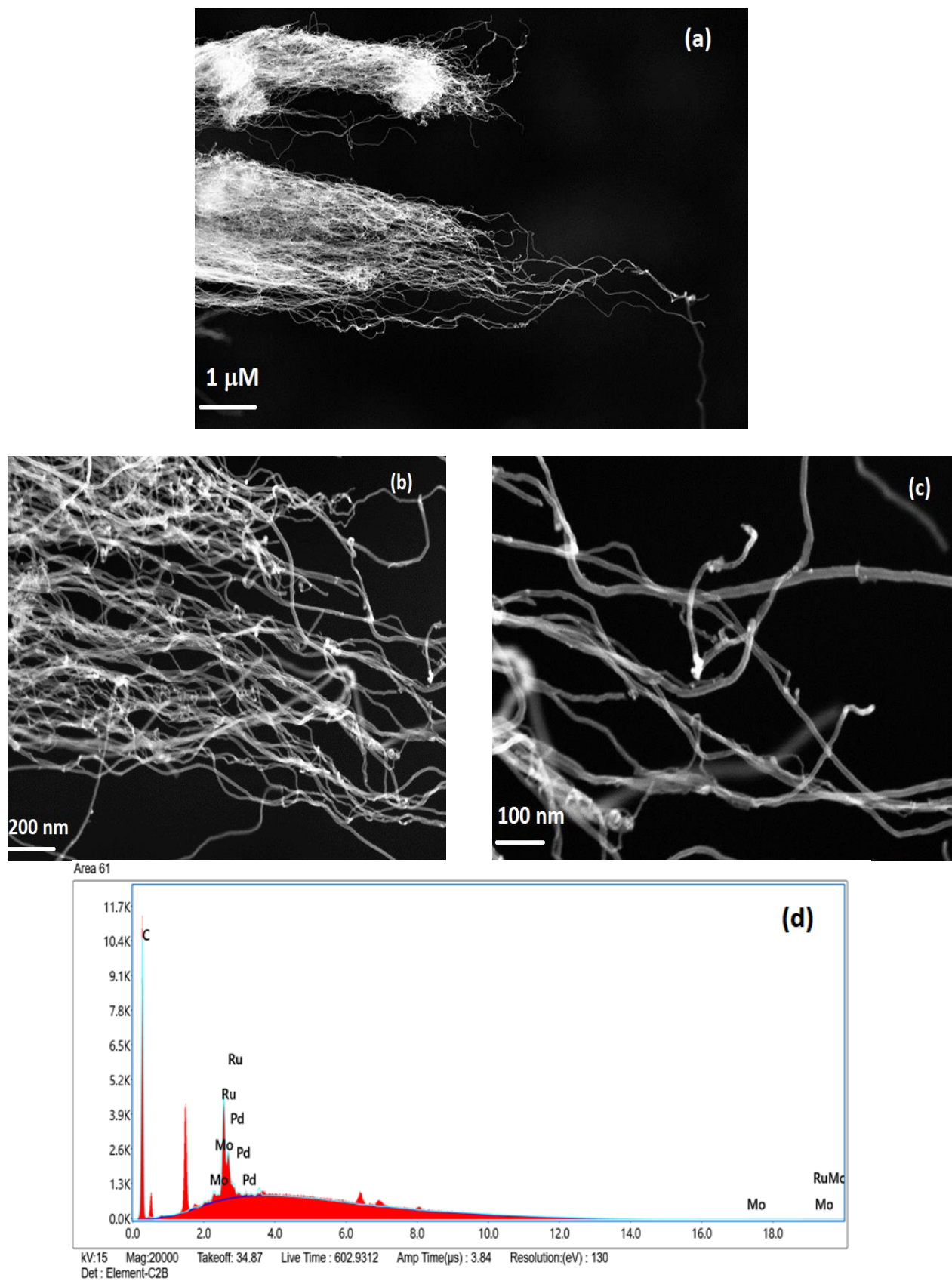


Figure 2. SEM images at different resolutions as (a) 1 μm, (b) 200 nm, (c) 100 nm and (d) EDX spectrum for 3% Ru-Mo-Pd/MWCNT catalyst.

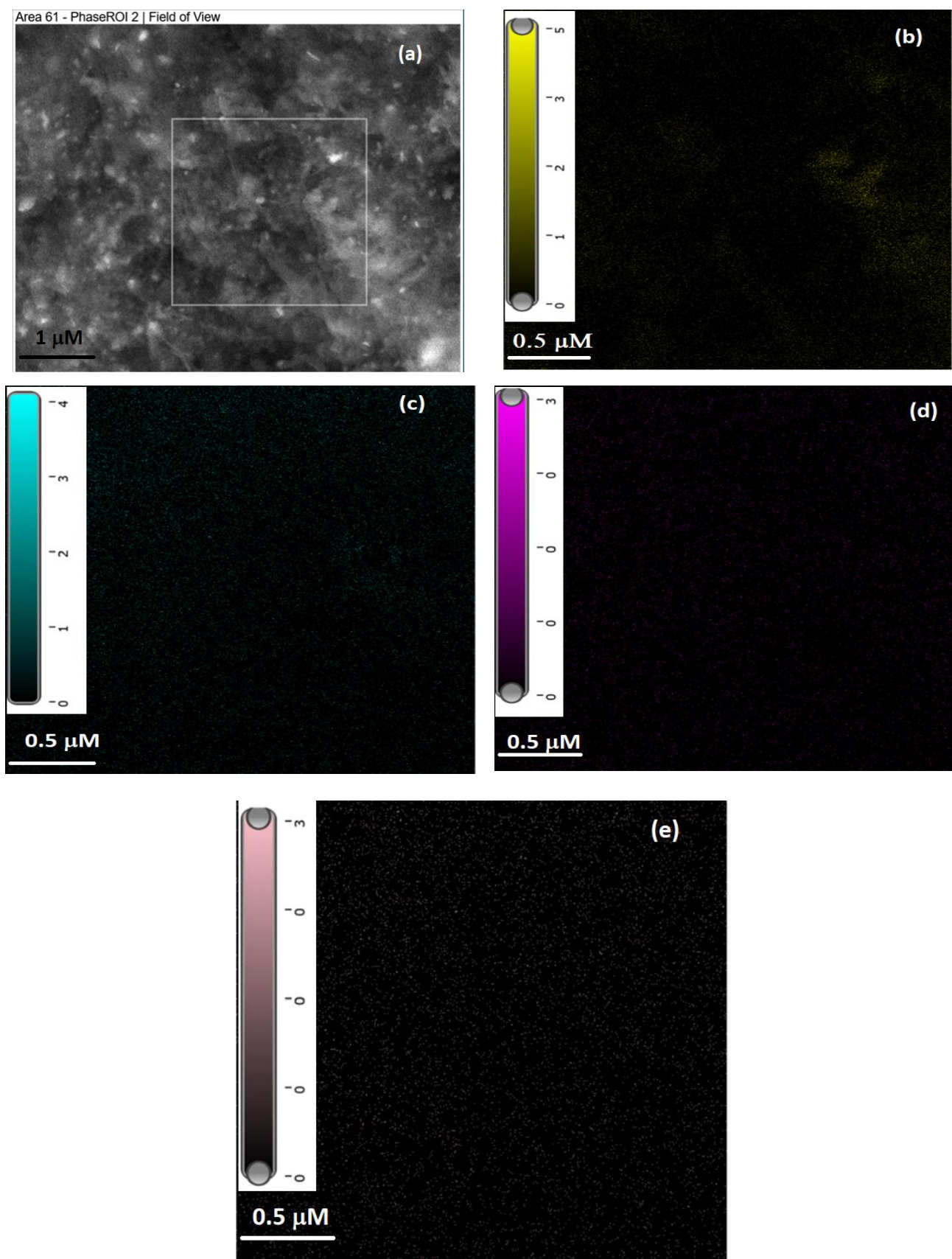


Figure 3. (a) SEM image of the area field EDX mapping taken and EDX elemental mapping of (a) area field (b) C1K (c) RuL (d) MoL (e) PdL for 3% Ru-Mo-Pd/MWCNT catalyst

3.2 Electrochemical measurements

Trimetallic Ru-Mo-Pd/MWCNT catalysts were prepared, characterized, and examined for detection of Cys via electrochemical methods. For the construction of electrodes, GCEs were modified with the trimetallic Ru-Mo-Pd/MWCNT catalysts. Firstly, Cys electrooxidation measurements were carried out by CV in 0.1 M pH 7.2 phosphate buffer solution. The Cys electrooxidation measurements in the absence and presence of 5 mM Cys in N₂-saturated 0.1 M pH 7.2 phosphate buffer solution at scan rate of 100 mVs⁻¹ are presented in Figure 4. The Cys electrooxidation peaks were observed at -0.2 V for Ru-Mo-Pd catalysts prepared at 0.0019-0.0076 mM Pd concentrations and the current density of these peaks increases with the increasing amount of electrodeposited Pd. This peak could be attributed to the Cys electrooxidation peak which was described in literature [53]. Pazalja and coworkers reported that multi-walled carbon nanotubes to Ru(III) complex modified glassy carbon and screen printed carbon electrodes gives increased current signals at around 0.2 V [53]. Furthermore, it is clear that further increases in the Pd amount to 0.0152 mM led to a shift this onset potential to more negative potentials of -0.4 V and current density increased significantly. It is clear that Cys was also effectively oxidized on GCE modified with trimetallic Ru-Mo-Pd/MWCNT catalysts. As a result, Ru-Mo-Pd/MWCNT prepared at 0.0152 mM Pd concentration exhibited remarkable enhanced catalytic current greater than the current peak of other Ru-Mo-Pd catalysts. The Cys concentration effect on Cys electrooxidation activity of Ru-Mo-Pd catalyst prepared at 0.0152 mM Pd was examined with different Cys concentrations of 0-50 mM in phosphate buffer solution by CV. These measurements are depicted in Figure 5. Results clearly reveal that current increased stepwise with successive additions of Cys, ascribed to the sensitive and rapid response to the Cys oxidation of the electrodes.

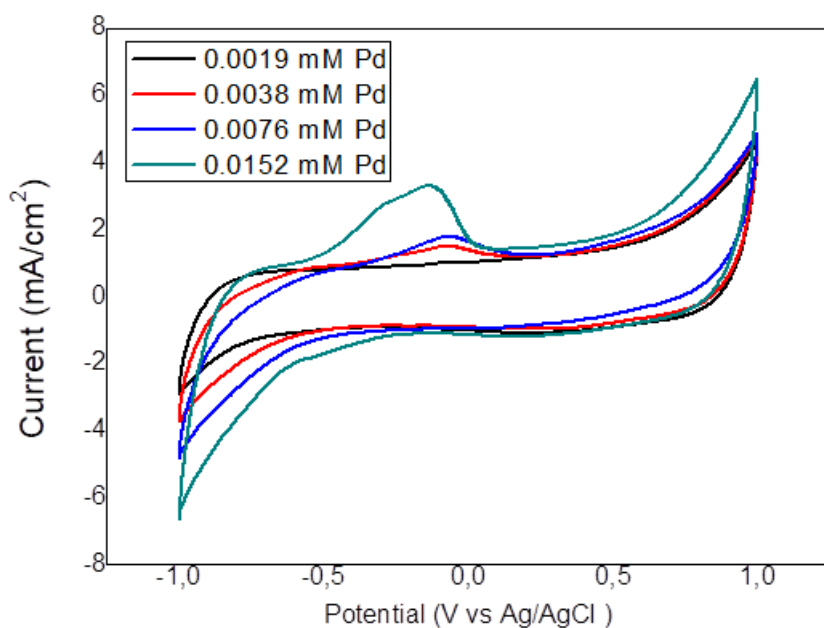


Figure 4. CVs with scan rate of 100 mV. s⁻¹ in the presence and absence of 10 mM Cys on Ru-Mo-Pd/MWCNT catalysts prepared at 0.0019 mM-0.0152 mM Pd concentrations

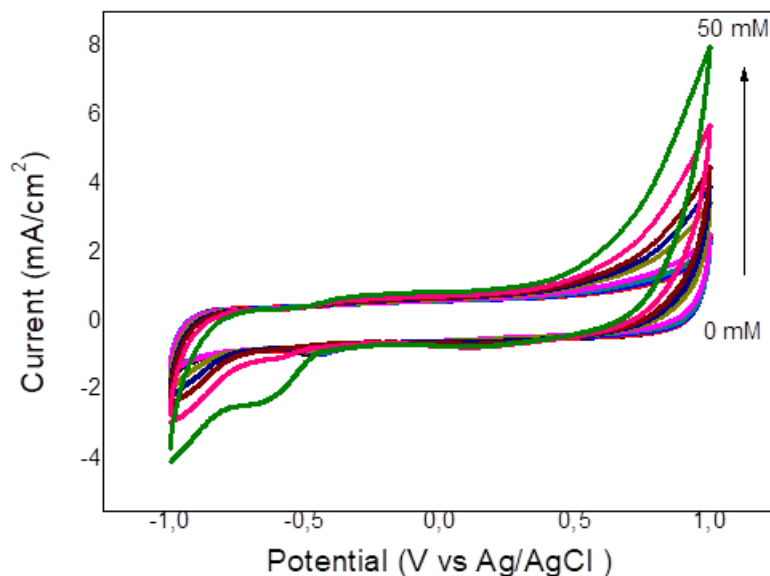


Figure 5. CVs of GC electrode modified with Ru-Mo-Pd/MWCNT prepared at 0.0152 mM in 0.1 M PBS (pH 7.4) containing different concentrations at 0, 0.1, 1, 5, 7, 10, 20, 50 mM of Cys; scan rate: 100 mV. s⁻¹

The pH effect of PBS was examined on the electrocatalytic activity of Cys using 3% Ru-Mo-Pd/MWCNT-modified GCE. Therefore, PBS prepared at different pHs (5.5, 7.2, 10) was introduced into the cell, 5 mM Cys was added and saturated with N₂ gas. The results of these measurements are given in Figure 6. It was observed that maximum current was obtained at pH=10. From this point, the rest of the measurements were carried out at pH=10.

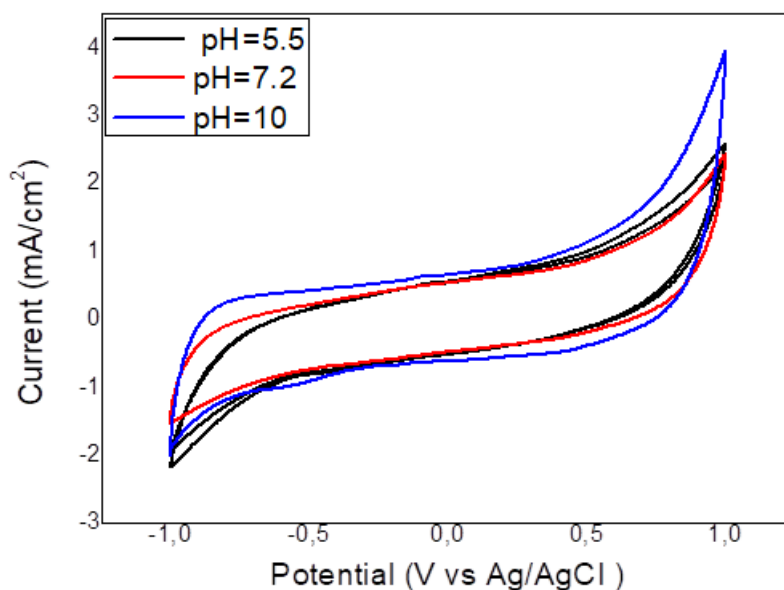


Figure 6. The effect of pH on Cys electro-oxidation using Ru-Mo-Pd/MWCNT catalyst prepared at 0.0152 mM.

The effect of scan rate on the electrocatalytic activity of Cys was investigated with Ru-Mo-Pd/MWCNT-modified GCE in 0.1 MPBS (pH=10) + 5 mM Cys and results of these measurements are illustrated in Figure 7. It was observed that Cys electro-oxidation current increased with increasing scan rate, representing a good linear relationship. This is ascribed to the fact that this reaction is controlled by diffusion.

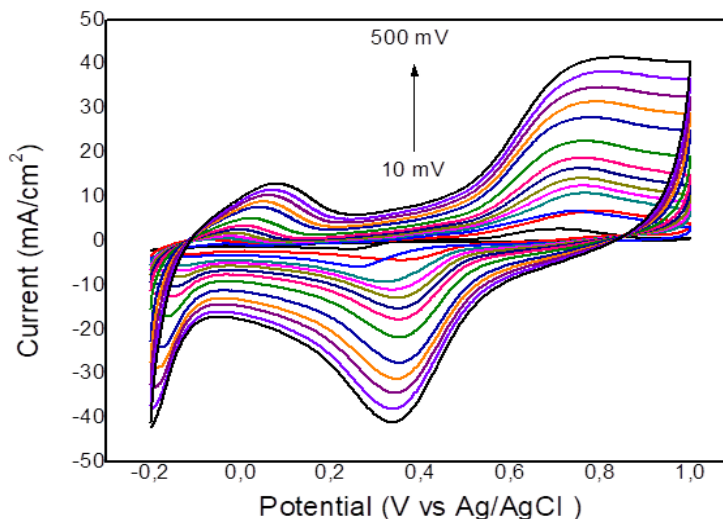


Figure 7. CV of GCE modified with Ru-Mo-Pd/MWCNT prepared at 0.0152 mM under different scan rates (10, 30, 50, 100, 120, 200, 230, 250, 300, 350, 400, 480, 500 $\text{mV} \cdot \text{s}^{-1}$) in 0.1 MPBS (pH=10) + 5 mM Cys.

The DPV method was utilized to determine the sensitivity of Ru-Mo-Pd/MWCNT-modified GCE as Cys sensor. The DPV curves of 3% Ru-Mo-Pd/MWCNT-modified GCE in 0.1 MPBS (pH=10) at varying Cys concentrations (0-1000 mM Cys) are presented in Figure 8a. The calibration curve was obtained by employing DPV results. Current densities against Cys concentrations were plotted and are also illustrated in Figure 8b. By the subsequent addition of Cys, one could observe that the current density of peaks observed at 0.2 V increases and peak potential shift to more negative values. This phenomenon could be attributed to the fact that the increase in the Cys concentration led to the decreased the kinetic resistance. It is clear that the calibration plot exhibited a linear relationship within the range of 5–200 μM with current sensitivity 0.136 $\mu\text{A} / \mu\text{M}$ (1926.3 $\mu\text{A}/\text{mMcm}^2$), higher than those reported in literature [1-5]. Limit of blank (LOB) and lowest detection limit (LOD) for Cys were measured with acceptable statistical certainty and lowest concentration of analyte, called the limit of quantification (LOQ), was determined with acceptable sensitivity for Ru-Mo-Pd/MWCNT-modified GCE. To determine LOB, 10 blank electrode responses without analyte were used. LOB, LOD, and LOQ were 0.08, 0.106, and 0.33 μM at (S/N=3), respectively. It is clear that the LOD of this Cys sensor is lower than the Cys sensors reported in the literature [1-9]. This sensor has a wide linear response within the range of 5–200 μM with high current sensitivity 0.136 $\mu\text{A}/\mu\text{M}$ and 0.1 μM as lowest detection limit at (S/N=3) signal to noise ratio. Interference studies reveal that Ru-Mo-Pd/CNT sensor is not affected by common interfering species.

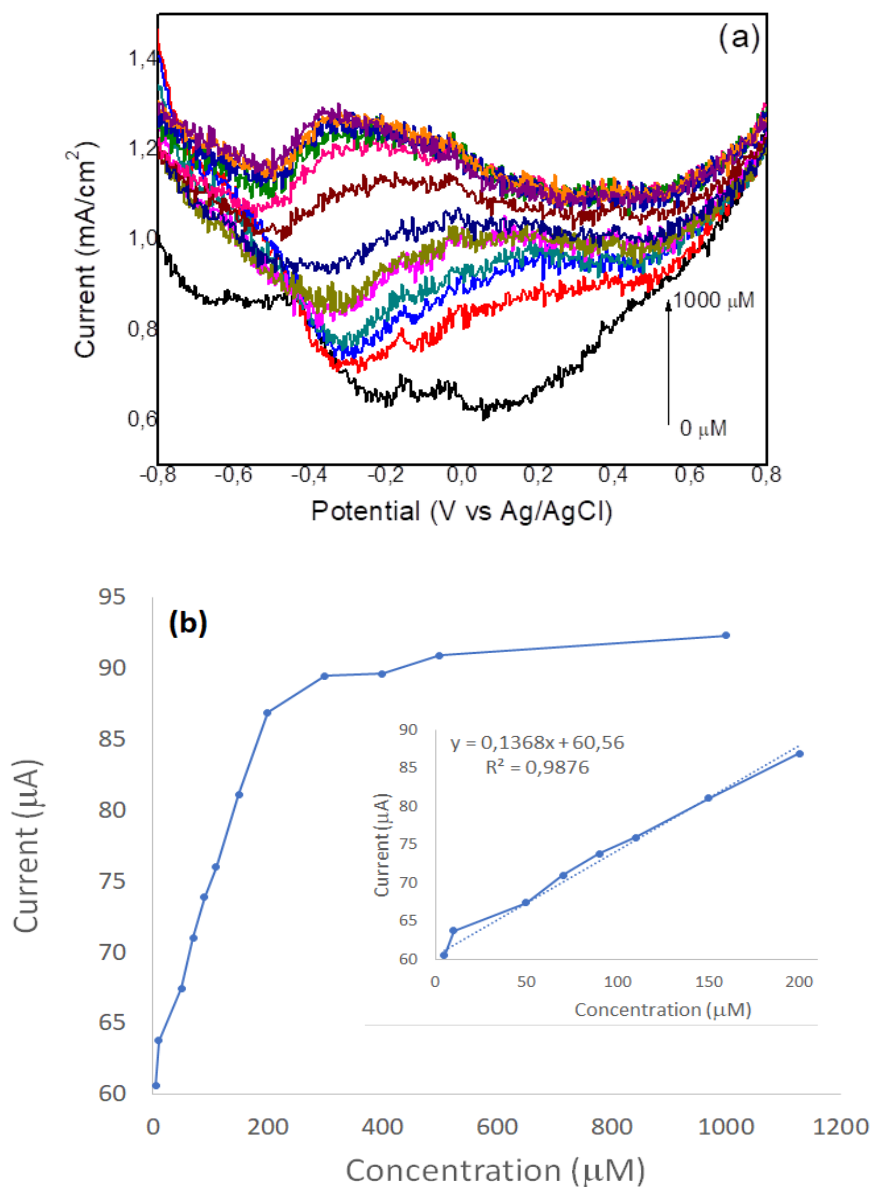


Figure 8. (a) DPV curves obtained at 10, 50, 70, 90, 110, 150, 200, 300, 400, 500, 1000 μM Cys concentrations for Ru-Mo-Pd/MWCNT GCE in 0.1 MPBS (pH=10) (b) calibration curves obtained from DPV maximum current values vs corresponding Cys concentration and insert graph shows the linear range 60-90 μA range.

This novel study reports a strategy to sense Cys on Ru/CNT modified GCE electrode. In Table 1, sensitivity, linear range, and LOD values from literature studies are given. As reported in Table 1, Ahmad and coworkers [1] employed elbow shaped Sb-doped ZnO nanowires synthesized by thermal evaporation as Cys sensor with $400 \text{ nA}\mu\text{M}^{-1}$ sensitivity 0.025 μM detection limit 0.075-100 μM detection limit. Xiao et al. [2] used manganese dioxide-carbon ($\text{MnO}_2\text{-C}$) nanocomposite as Cys sensor and obtained good linear relationship with that of the L-Cys concentration in the range of 0.5–680 μM ($R = 0.9986$), with a low detection limit of 22 nM. At another study Cu^{2+} /MWNTs-PVP Cys sensing ability was examined and $7.0 \text{ nA}/\mu\text{M}$ sensitivity and with 5–60 μM linear range [3]. One could note that when CoTAPc/MWCNTs were employed as Cys electrochemical sensor and results revealed that this

material was good electrochemical sensor with a limit of detection of $2.8 \cdot 10^{-7}$ M with 100 nA/ μ M [4]. In literature, MoS₂/PDDA-MC was also reported as Cys electrochemical sensor with 738.6 nA/ μ M sensitivity and 45–155 μ M linear range [5]. As has been reported in this work, Ru-Mo-Pd/CNT material used as Cys electrochemical sensor and sensitivity obtained as 136 nA/ μ M with 5–200 μ M linear range and 0.1 μ M LOD value. As can be seen, the analytical parameters are comparable or better than the results reported for Cys determination at the surface of other modified electrodes [1-5, 54-57]. It is clear that this sensor has a good sensitivity and broader linear range compared literature studies [1-5, 54-57].

Table 1. Electrode materials employed for electrochemical determination of Cys.

Sensor	Sensitivity	Linear range	LOD	Ref
Sb-doped ZnO nanowires	400 nA/ μ M	0.075-100 μ M	0.025 μ M	[1]
Cu ²⁺ /MWNTs-PVP	7.0 nA/ μ M	5–60 μ M		[3]
CoTAPc-MWNTs	100 nA/ μ M	5-40 μ M		[4]
MnO ₂ -MWCNTs	-	0.5–680 μ M		[2]
MoS ₂ /PDDA-MC	738.6 nA/ μ M	0.45–155 μ M		[5]
Boron_doped diamond electrode	-	1–200 μ M	0.9 μ M	[54]
Poly(3,3_ethylendioxythiophene) modified screen printed electrodes	-	0.05–200 μ M	0.03 μ M	[55]
Carbon electrode bulk modified with cobalt phthalocyanine	-	1–12 μ M	0.2 μ M	[56]
Carbon ceramic with ruthenium complex	-	5–685 μ M	1 μ M	[57]
Ru-Mo-Pd/CNT	136 nA/μM (0.136 μA/μM)	5–200 μM	0.1 μM	This work

Surface properties of electrode materials such as diffusion properties, electrode capacitance, and charge transfer kinetics can be easily determined by EIS. The Nyquist graph of the electrochemical impedance spectrum consists of semi-circular and linear sections. The semicircular part gives the charge transfer and the linear part corresponds to the controlled diffusion process. For Ru-Mo-Pd/MWCNT-modified GCE, electrochemical impedance behavior was determined by using the EIS technique in 0.1 M PBS (pH=10) + 5 mM Cys. Fig. 9 depicts the electrochemical impedance behavior of Ru-Mo-Pd/MWCNT-modified GCE obtained at different potentials in 0.1 MPBS (pH=10) + 5 mM Cys. Cys electro-oxidation on Ru-Mo-Pd/MWCNT-modified GCE at various potentials has different electrochemical impedance behaviors and the large arc reveals that the Cys electrooxidation has slow kinetics but the small arc is a sign of fast Cys electrooxidation kinetics. There is a decrease in the arc diameter with increasing potential and the lowest arc was obtained at 0.6 V, attributed to the fact that the

charge transfer resistance of the Cys electro-oxidation reaction reduces. Ru-Mo-Pd/MWCNT-modified GCE exhibited surface resistance at 0.6 V with a 70-ohm R_{ct} value, which is smaller than the other potential values.

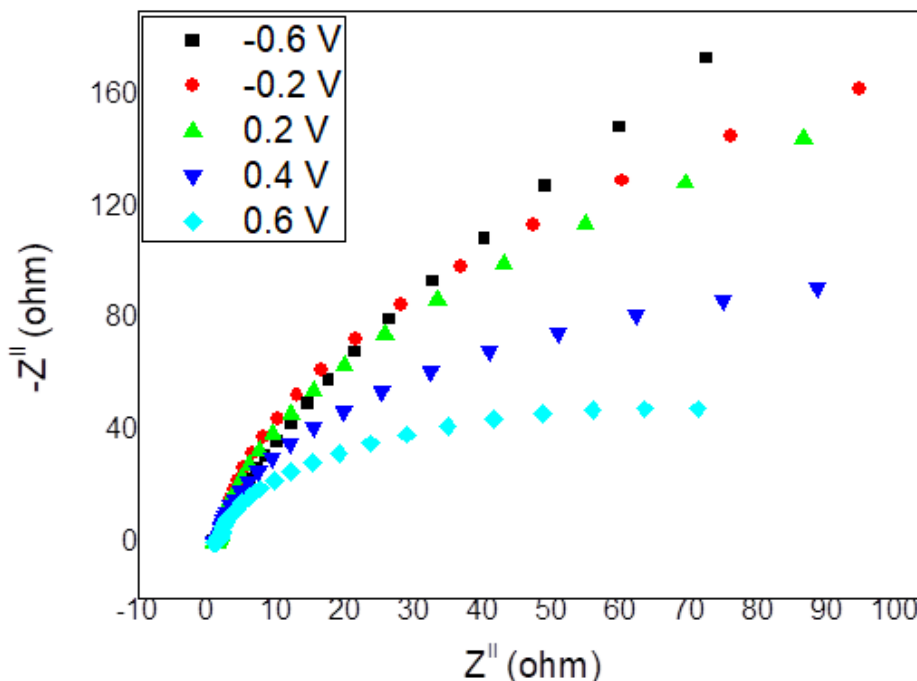


Figure 9. Electrochemical impedance spectra for Ru-Mo-Pd/MWCNT-modified GCE at different potentials in 0.1 M PBS (pH=10) + 5 mM Cys. Frequency range (0.02–100,000 Hz), signal amplitude (10 mV).

Interference measurements on the Ru-Mo-Pd/MWCNT-modified GCE sensor were carried out including some possible interfering species such as D-glucose, uric acid, L-Tyrosine, L-Tryptophane, and H_2O_2 from blood samples through the determination of Cys. These measurements were carried out by CV and EIS at 0.6 V potential. CVs of these interfering species were depicted in Figure 10a. It was observed that the interference effect of H_2O_2 and L-Cysteine was higher than uric acid, D-glucose, tryptophane, and tyrosine. Likewise, EIS measurements revealed that EIS results are in agreement with results showing that L-Cysteine had the lowest charge transfer (Figure 10b). In this context, it is clear that the current and impedance responses of interfering species are small enough to ignore, revealing that Ru-Mo-Pd/MWCNT-modified GCE has excellent selectivity for Cys determination.

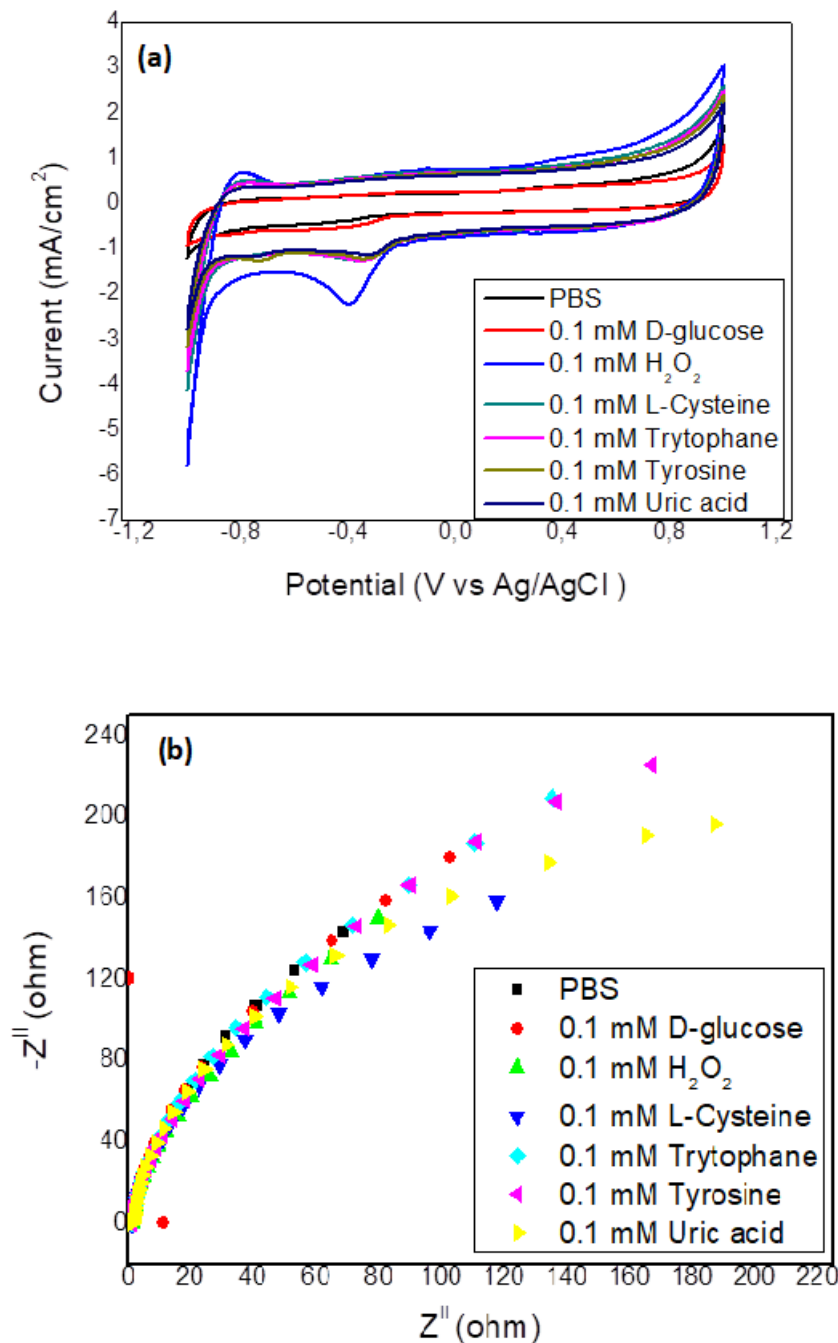


Figure 10. (a) CV voltammogram (b) EIS at 0.6 V for interfering substances on the Ru-Mo-Pd/MWCNT-modified GCE

Finally, real sample measurements were carried out on Ru-Mo-Pd/MWCNT-modified GCE by the standard addition method. To measure real samples, 600 mg tablets of acetylcysteine were powdered and homogenized and following this, 1 mg acetylcysteine was transferred into a 50 mL volumetric flask containing 0.1 M PBS solution at pH=10. Employing this stock solution, 1.5 mM acetylcysteine was prepared by diluting this solution and the response of the sensor was obtained in this solution. Then, 1.5 mM of acetylcysteine was added to the real sample solution and the response of the sensor was recorded again. As given in Table 2, the recovery values are acceptable. The relative standard deviation of the

sample for six successive detections is less than 5%. This study showed that the Ru-Mo-Pd/MWCNT-modified GCE exhibited good performance in real samples.

Table 2. Cys analysis data for acetylcysteine drug sample

Sample	Added (mM)	Found (mM)	Recovery (%)
1	1.5	1.45	96.70
2	3.0	3.10	96.70
3	6.0	5.85	97.50

4. CONCLUSIONS

The Ru-Mo-Pd/MWCNT catalyst was prepared in two steps. First of all, Ru-Mo/MWCNT catalyst was synthesized by the NaBH₄ reduction method. Following this, Ru-Mo/MWCNT-modified GCE was prepared and Pd electrodeposition at varying Pd concentrations was carried out to obtain Ru-Mo-Pd/MWCNT catalysts. It was observed that the Ru-Mo-Pd/MWCNT catalyst at 0.0152 mM Pd concentration had the highest Cys electrooxidation activity. Thus, further measurements, such as determining sensitivity, limit of detection, interference study, and real sample measurement, were carried out with this catalyst at pH=10. Ru-Mo-Pd/MWCNT catalyst at 0.0152 mM Pd concentration was characterized by TEM and SEM-EDX. Characterization results revealed that the Ru-Mo-Pd/MWCNT catalyst was successfully synthesized. Ru-Mo-Pd/MWCNT-modified GCE had good electrocatalytic responses to Cys with high sensitivity, stability, and selectivity. Ru-Mo-Pd/MWCNT-modified GCE could effectively resist the effect of interfering species such as D-glucose, uric acid, L-Tyrosine, L-Tryptophane, and H₂O₂, which are common interfering species. This study is novel and one of the few studies in the literature to construct a Cys sensor from nanomaterials to detect Cys effectively.

ACKNOWLEDGEMENTS

The authors would like to thank the Scientific and Technological Research Council of Turkey for financial support of chemicals and characterization in TUBITAK projects (project nos: 114M879, 114M156, 116M004). Kadir Selçuk and Omer Faruk Er thank the Council of Higher Education (YOK) for 100/2000. In addition, Omer Faruk Er is grateful to TUBITAK 2211 A for scholarships.

References

- 1 M. Ahmad, C. F. Pan, and J. Zhu, *J. Mater. Chem.*, 20 (2010) 7169.
- 2 C. H. Xiao, J. H. Chen, B. Liu, X. C. Chu, L. A. Wu, S. Z. Yao, *Phys. Chem. Chem. Phys.*, 13 (2011) 1568.
- 3 C. Silva, M. C. Breitzkreitz, M. Santhiago, C. C. Correa, L. T. Kubota, *Electrochim. Acta*, 71 (2012) 150.
- 4 S. Nyoni, T. Mugadza, T. Nyokong, *Electrochim. Acta*, 128 (2014) 32.
- 5 Z. X. Zheng, Q. L. Feng, J. Li, C. M. Wang, *Sens. Actuators, B.*, 221 (2015) 1162.
- 6 M. Pazalja, E. Kahrovic, A. Zahirovic, E. Turkusic, *Int. J. Electrochem. Sci.*, 11 (2016) 10939.

- 7 J. Yao, C. H. Liu, L. Liu, M. Chen, M. Yang, *J. Electrochem. Soc.*, 165 (2018) B551.
- 8 M. Heidari, A. Ghaffarinejad, *Microchim. Acta*, 186 (2019), 365.
- 9 A. Kurniawan, F. Kurniawan, F. Gunawan, S. H. Chou, M. J. Wang, *Electrochim. Acta*, 293 (2019) 318.
- 10 M. Duff, *Manuf. Chem.*, 53 (1982) 51.
- 11 J. C. Crawhall, *Clin. Biochem.*, 18 (1985) 139.
- 12 L. A. Bobek, M. J. Levine, *Crit. Rev. Oral. Biol. Med.*, 4 (1993) 251.
- 13 J. Kos, T. T. Lah, *Oncol. Rep.*, 5 (1998) 1349.
- 14 A. D. Marshall, J. F. Derbyshire, P. McPhie, W. B. Jakoby, *Chem. Biol. Interact.*, 109 (1998), 109.
- 15 K. Atacan, *J. Alloy. Compd.*, 791 (2019) 391.
- 16 M. H. Stipanuk, *Neurochem. Res.*, 29 (2004) 105.
- 17 A. Adachi, Y. Sarayama, H. Shimizu, Y. Yamada, T. Horikawa, *Br. J. Dermatol.*, 153 (2005) 226.
- 18 J. Velisek, K. Cejpek, *Czech J. Food Sci.*, 24 (2006) 45.
- 19 C. O. Meese, D. Specht, D. Ratge, M. Eichelbaum, H. Wisser, *Fresenius J. Anal. Chem.*, 346 (1993) 837.
- 20 K. Kargosha, S. H. Ahmadi, M. Zeeb, S. R. Moeinossadat, *Talanta*, 74 (2008) 753.
- 21 P. Rezanka, J. Koktan, H. Rezankova, P. Matejka, V. Kral, *Colloids & Surfaces A* ., 436 (2013) 961.
- 22 S. Rastegarzadeh, F. Hashemi, *Anal. Methods*, 7 (2015) 1478.
- 23 N. Pan, L. Y. Wang, L. L. Wu, C. F. Peng, Z. J. Xie, *Microchim. Acta*, 184 (2017) 65.
- 24 H. H. Rao, Y. Li, G. L. Zhang, Z. H. Xue, G. H. Zhao, S. Y. Li, X. Z. Du, *Bull. Korean Chem. Soc.*, 38 (2017) 1023.
- 25 Z. L. Huang, Y. F. Yang, Y. J. Long, H. Z. Zheng, *Anal. Methods*, 10 (2018) 2676.
- 26 J. Zhu, B. Z. Zhao, Y. Qi, J. J. Li, X. Li, J. W. Zhao, *Sens. Actuators, B.*, 255 (2018) 2927.
- 27 L. R. Liu, G. B. Zhu, W. Zeng, Y. H. Yi, B. H. Lv, J. J. Qian, D. P. Zhang, *Microchim. Acta*, 186 (2019) 98.
- 28 H. Tavallali, G. Deilamy-Rad, N. Mosallanejad, *Appl. Biochem. Biotechnol.*, 187 (2019) 913.
- 29 F. Salman, H. C. Kazici, H. Kivrak, *Front. Chem. Sci. Eng.*, 14 (2020) 629.
- 30 H. Kivrak, O. Alal, D. Atbas, *Electrochim. Acta.*, 176 (2015) 497.
- 31 H. C. Kazici, F. Salman, H. D. Kivrak, *Mater. Sci.-Pol.*, 35 (2017) 660.
- 32 O. Sahin, H. Kivrak, A. Kivrak, H. C. Kazici, O. Alal, D. Atbas, *Int. J. Electrochem. Sci.*, 12 (2017) 762.
- 33 H. C. Kazici, A. Caglar, T. Aydogmus, N. Aktas, H. Kivrak, *J. Colloid Interface Sci.*, 530 (2018) 353.
- 34 O. Alal, A. Caglar, H. Kivrak, O. Sahin, *Electroanalysis*, 31 (2019) 1646-1655.
- 35 A. Caglar, H. C. Kazici, D. Alpaslan, Y. Yilmaz, H. Kivrak, N. Aktas, *Fuller. Nanotub. Car. N.* 27 (2019) 736.
- 36 H. C. Kazici, M. Yayla, B. Ulas, N. Aktas, H. Kivrak, *Electroanalysis*, 31 (2019) 1118.
- 37 H. D. Kivrak, N. Aktas, A. Caglar, *Int J Nano Dimens.* 10 (2019) 252.
- 38 N. A. Ertas, E. Kavak, F. Salman, H. C. Kazici, H. Kivrak, A. Kivrak, *Electroanalysis*, 32 (2020) 1178.
- 39 B. Ulas, A. Caglar, S. Yilmaz, U. Ecer, Y. Yilmaz, T. Sahan, H. Kivrak, *Int. J. Energy Res.*, 43 (2019) 8985.
- 40 C. Avci, F. Cicek, H. C. Kazici, A. Kivrak, H. Kivrak, *Int. J. Nano Dimens.*, 9 (2018) 15.
- 41 A. Bulut, M. Yurderi, O. Alal, H. Kivrak, M. Kaya, M. Zahmakiran, *Adv. Powder Technol.*, 29 (2018) 1409.
- 42 A. Caglar, T. Sahan, M. S. Cogenli, A. B. Yurtcan, N. Aktas, H. Kivrak, *Int. J. Hydrogen Energy*, 43 (2018) 11002.

- 43 H. Kivrak, D. Atbas, O. Alal, M. S. Cogenli, A. Bayrakceken, S. O. Mert, O. Sahin, *Int. J. Hydrogen Energy*, 43 (2018) 21886.
- 44 B. Ulas, A. Caglar, O. Sahin, H. Kivrak, *J. Colloid Interface Sci.*, 532 (2018) 47.
- 45 B. Ulas, A. Kivrak, N. Aktas, H. Kivrak, *Fuller. Nanotub. Car. N. 27* (2019) 545.
- 46 B. Ulas, A. Caglar, H. Kivrak, *Int. J. Energy Res.*, 43 (2019) 3436.
- 47 O.Sahin, H. Kivrak, M. Karaman, D. Atbas, *Am. J. Mater. Sci.*, 3 (2015) 15.
- 48 A. Caglar, M. S. Cogenli, A. B. Yurtcan, H. Kivrak, *Renewable Energy*, 150 (2020) 78.
- 49 O. F. Er, A. Caglar, B. Ulas, H. Kivrak, A. Kivrak, *Mater. Chem. Phys.*, 241 (2020) 122422.
- 50 B. Ulas, A. Caglar, A. Kivrak, N. Aktas, H. Kivrak, *Ionics*, 26 (2020) 3109.
- 51 TA Hansu, A Caglar, O Sahin, H Kivrak, *Mater. Chem Phys.*, 239 (2020) 239, 122031.
- 52 B. Ulas, H. Kivrak, *Gen. Chem.*, 6 (2020) 190028.
- 53 M. Pazalja , E. Kahrović , A. Zahirović , E. Turkušić, *Int J Electrochem Sci.* 11 (2016) 10939.
- 54 N. Spataru, B.V. Sarada, E. Popa, D.A. Tryk, A. Fujishima, *Anal. Chem.*, 73 (2001) 514.
- 55 W. Y. Su, S.H. Cheng, *Electrochem. Commun.*, 10(2008) 899.
- 56 B. Filanovsky, *Anal. Chim. Acta.*, 394 (1999) 91.
- 57 A. Salimi, R. Hallaj, M.K. Amini, *Anal. Chim. Acta*, 534 (2005) 335.

© 2021 The Authors. Published by ESG (www.electrochemsci.org). This article is an open access article distributed under the terms and conditions of the Creative Commons Attribution license (<http://creativecommons.org/licenses/by/4.0/>).